

Dislocation Field Theory in 2D: Application to Graphene

Markus Lazar^{a,b,*}

^a Heisenberg Research Group,
Department of Physics,
Darmstadt University of Technology,
Hochschulstr. 6,
D-64289 Darmstadt, Germany

^b Department of Physics,
Michigan Technological University,
Houghton, MI 49931, USA

October 15, 2015

Abstract

A two-dimensional (2D) dislocation continuum theory is being introduced. The present theory adds elastic rotation, dislocation density, and background stress to the classical energy density of elasticity. This theory contains four material moduli. Two characteristic length scales are defined in terms of the four material moduli. Non-singular solutions of the stresses and elastic distortions of an edge dislocation are calculated. It has been pointed out that the elastic strain agrees well with experimental data found recently for an edge dislocation in graphene.

Keywords: dislocations; field theory; graphene; length scales; elastic deformation.

**E-mail address:* lazar@fkp.tu-darmstadt.de (M. Lazar).

1 Introduction

A challenging and active research field is the investigation of the material behaviour of graphene, especially the study of dislocations in graphene (see, e.g., [2, 3, 4, 5, 6]). Graphene is a two-dimensional (2D) material with extraordinary physical properties. In a recent experiment [1], the elastic strain and rotation fields produced by an edge dislocation in graphene have been observed for the first time. It was reported that the lattice rotation is quite appreciable at the dislocation core. Also it was noted that the measured elastic strain contours, do not agree with the corresponding contours calculated in classical elasticity theory. This indicates that a general dislocation continuum theory including the elastic rotation, is needed for a theoretical prediction of realistic strain and rotation contours. Dislocations are critical for understanding plasticity in 2D crystals and predicting mechanical properties. Dislocations are the fundamental carrier of plasticity of materials and little is known about their effect in 2D crystals.

This paper shows that the so-called dislocation field or dislocation gauge theory (see, e.g., [7, 8, 9, 10, 11, 12, 13, 14]) is a promising and excellent candidate to fulfill the requirements mentioned above, and to give contours which agree with experimental data. In [11] a dislocation field theory, which can be considered as the dislocation gauge theory of the three-dimensional translation group $T(3)$ was developed. The idea of a static dislocation field theory, is to use three terms in the general distortion energy density. One term contains the elastic strain and the elastic rotation fields. Another one proportional to the dislocation density tensor having the meaning of dislocation core energy density and a term containing a background stress tensor, which is needed for self-equilibrating of the dislocations. It is important to mention that the force stress tensor is not symmetric anymore. In [11], non-singular solutions for screw and edge dislocations were found. This paper adopts the framework of [11] in order to formulate a dislocation field theory for two-dimensional materials, which is a gauge theory of the two-dimensional translation group $T(2)$. We suggest using such a dislocation field theory as a 2D dislocation continuum theory for dislocations in graphene. We propose a 2D dislocation field theory, because the strain fields around dislocations differ from those given by classical elasticity with line singularities.

The outline of this paper is as follows. In Section 2, the fundamental framework of 2D dislocation continuum field theory is presented. In Section 3, the non-singular solutions of the stress and elastic distortion fields are given. In addition, the components of the dislocation density vector and the effective Burgers vector are calculated. The physical features of the obtained solutions are presented in suitable plots. Section 4, concludes our work.

2 Basic Framework

In 2D a dislocation is characterized by the Burgers vector which can be in x - and y -directions with components b_x and b_y . There is no z -direction in 2D. For that reason a dislocation in 2D is a point dislocation. The dislocation is located at the dislocation point. In real 2D materials only edge dislocations are possible since the Burgers vector is

constrained to lie in the xy -plane. The two physical state quantities in the static theory of dislocations are the elastic distortion tensor

$$\beta_{ij} = u_{i,j} - \beta_{ij}^P, \quad i, j = x, y \quad (1)$$

and the dislocation density vector

$$\alpha_i = \epsilon_{kl} \beta_{il,k}, \quad (2)$$

$$\alpha_i = -\epsilon_{kl} \beta_{il,k}^P, \quad (3)$$

which is the measure how much the elastic distortion tensor β_{ij} and the plastic distortion tensor β_{ij}^P are incompatible. $\epsilon_{ij} = -\epsilon_{ji}$, $\epsilon_{xy} = 1$ is the totally antisymmetric second rank tensor. The displacement vector is denoted by u_i and is not a physical state quantity. Since in 2D a dislocation is a point dislocation, there is no Bianchi identity for dislocations unlike 3D where a dislocation is a line defect. Also it holds

$$T_{ijk} = \epsilon_{jk} \alpha_i = \beta_{ik,j} - \beta_{ij,k}, \quad \alpha_i = \frac{1}{2} \epsilon_{jk} T_{ijk}, \quad (4)$$

where T_{ijk} is Cartan's torsion tensor in 2D (see, e.g., [15]).

The deformation energy density consists of three pieces

$$W = W_{\text{el}} + W_{\text{di}} - W_{\text{bg}}. \quad (5)$$

The first piece is the elastic distortion energy density

$$W_{\text{el}} = \frac{1}{2} \sigma_{ij} \beta_{ij}, \quad (6)$$

the second piece is the dislocation energy density

$$W_{\text{di}} = \frac{1}{2} H_i \alpha_i, \quad (7)$$

playing the role of the dislocation core density and finally, the third piece is the background part

$$W_{\text{bg}} = \sigma_{ij}^0 \beta_{ij}, \quad (8)$$

containing the contribution of the residual or background stress tensor σ_{ij}^0 , fulfilling the condition $\sigma_{ij,j}^0 = 0$, needed to equilibrate dislocations.

The specific response fields in the framework of dislocation field theory shall be given for an isotropic, linearly elastic medium. The force stress tensor is defined by

$$\sigma_{ij} = \frac{\partial W_{\text{el}}}{\partial \beta_{ij}} = \lambda \delta_{ij} \beta_{kk} + 2\mu \beta_{(ij)} + 2\gamma \beta_{[ij]}, \quad (9)$$

where the symmetric part, $\beta_{(ij)} = (\beta_{ij} + \beta_{ji})/2$, is the elastic strain tensor and the skew-symmetric part, $\beta_{[ij]} = (\beta_{ij} - \beta_{ji})/2$, determines the elastic rotation. Here μ and λ are the

Lamé coefficients. The coefficient γ is an additional material parameter due to the skew-symmetric part of the elastic distortion (the elastic rotation). Thus, γ is the modulus of rotation (see also [11]). The skew-symmetric stress $\sigma_{[ij]}$ is caused by the (local) elastic distortion $\beta_{[ij]}$. In 2D the trace of the elastic distortion tensor is

$$\sigma_{kk} = \sigma_{xx} + \sigma_{yy} = 2(\lambda + \mu) \beta_{kk}, \quad (10)$$

due to $\delta_{kk} = 2$. The response to the dislocation density vector is given by

$$H_i = \frac{\partial W_{\text{di}}}{\partial \alpha_i} = c \alpha_i \quad (11)$$

and is the dislocation excitation vector. In 2D, the dislocation density vector is already irreducible with respect to the two-dimensional group of isotropy, $SO(2)$, and it possesses two independent vector components (α_x, α_y) (see, e.g., [15, 16]). c is the dislocation modulus. H_i has the physical meaning of a pseudo-moment stress vector (see also, [11]). Since in 2D we have a dislocation density vector, the theory possesses only one dislocation modulus unlike 3D where three dislocation moduli are present. This 2D dislocation continuum field theory contains four material constants: the two Lamé moduli μ and λ , the rotation modulus γ , and the dislocation modulus c . The positive semi-definiteness of W , $W \geq 0$, requires the restriction

$$\mu \geq 0, \quad \gamma \geq 0, \quad \mu + \lambda \geq 0, \quad c \geq 0. \quad (12)$$

The Euler-Lagrange equations of W with respect to the elastic distortion tensor are given by

$$\frac{\delta W}{\delta \beta_{ij}} = \frac{\partial W}{\partial \beta_{ij}} - \partial_k \frac{\partial W}{\partial \beta_{ij,k}} = 0, \quad (13)$$

which give the fundamental field equations for dislocations, the dislocation equilibrium condition. They read in terms of the response quantities

$$\epsilon_{jk} H_{i,k} + \sigma_{ij} = \sigma_{ij}^0 \quad (14)$$

and with Eq. (11)

$$c \epsilon_{jk} \alpha_{i,k} + \sigma_{ij} = \sigma_{ij}^0. \quad (15)$$

Differentiating Eq. (14) with respect to x_j , the force equilibrium condition of the force stress tensor σ_{ij} follows

$$\sigma_{ij,j} = 0. \quad (16)$$

By means of Eq. (2), Eq. (15) takes the following form

$$c(\beta_{ik,jk} - \beta_{ij,kk}) + \sigma_{ij} = \sigma_{ij}^0. \quad (17)$$

Using the inverse constitutive relation for β_{ij}

$$\beta_{ij} = \frac{\gamma + \mu}{4\mu\gamma} \sigma_{ij} + \frac{\gamma - \mu}{4\mu\gamma} \sigma_{ji} - \frac{\nu}{2\mu(1 + \nu)} \delta_{ij} \sigma_{kk}, \quad (18)$$

where the 2D Poisson ratio ν is expressed in terms of the Lamé coefficients

$$\nu = \frac{\lambda}{2\mu + \lambda}, \quad \lambda = \frac{2\mu\nu}{1 - \nu} \quad (19)$$

and the trace of the elastic distortion tensor, which gives the elastic dilatation,

$$\beta_{kk} = \beta_{xx} + \beta_{yy} = \frac{1 - \nu}{2\mu(1 + \nu)} \sigma_{kk}, \quad (20)$$

and Eq. (16), the field equation (17) can be rewritten in terms of the force stress tensor. The result reads

$$c \left[\frac{\gamma - \mu}{4\mu\gamma} \sigma_{ki,jk} - \frac{\nu}{2\mu(1 + \nu)} \sigma_{kk,ij} - \frac{\gamma + \mu}{4\mu\gamma} \sigma_{ij,kk} - \frac{\gamma - \mu}{4\mu\gamma} \sigma_{ji,kk} + \frac{\nu}{2\mu(1 + \nu)} \delta_{ij} \sigma_{ll,kk} \right] + \sigma_{ij} = \sigma_{ij}^0. \quad (21)$$

Eq. (21) is the fundamental field equation for dislocations in terms of the force stress tensor derived in the framework of dislocation field theory in 2D. Thus, Eq. (21) is the equation of motion for the stress tensor. Eq. (21) will serve exciting solutions for the dislocation fields.

It can be seen in Eq. (21) that the components of the force stress tensor σ_{ij} are coupled in that equation. We can construct two simple, uncoupled, inhomogeneous Helmholtz equations for the trace σ_{kk} , and the skew-symmetric part $\sigma_{[xy]}$. The trace of Eq. (21) gives

$$\left[1 - \frac{c}{2\mu(1 + \nu)} \Delta \right] \sigma_{kk} = \sigma_{kk}^0, \quad (22)$$

where Δ denotes the 2D Laplacian. From the skew-symmetric part of Eqs. (15) and (21) and some simple algebra, we obtain

$$\left[1 - \frac{c(\mu + \gamma)}{4\mu\gamma} \Delta \right] \sigma_{[xy]} = \sigma_{[xy]}^0. \quad (23)$$

3 Dislocation Fields

In this section, the field equation (21) will be solved. In order to satisfy the force equilibrium condition (16), the stress function ansatz of Mindlin-type [17, 11] should be used

$$\sigma_{ij} = \begin{pmatrix} \partial_{yy}^2 \Phi - \partial_{xy}^2 \Psi & -\partial_{xy}^2 \Phi + \partial_{xx}^2 \Psi \\ -\partial_{xy}^2 \Phi - \partial_{yy}^2 \Psi & \partial_{xx}^2 \Phi + \partial_{xy}^2 \Psi \end{pmatrix} \quad (24)$$

with the two stress functions Φ and Ψ . It holds: $\sigma_{kk} = \Delta\Phi$ and $\sigma_{[xy]} = \frac{1}{2}\Delta\Psi$. A similar stress function ansatz holds for the background stress σ_{ij}^0 in terms of the background stress functions Φ^0 and Ψ^0 (see Appendix A).

Substituting Eq. (24) into Eq. (21) or into Eqs. (22) and (23) gives two inhomogeneous Helmholtz equations for the stress functions

$$[1 - \ell_1^2 \Delta]\Phi = \Phi^0, \quad (25)$$

$$[1 - \ell_2^2 \Delta]\Psi = \Psi^0, \quad (26)$$

where the two characteristic lengths of the 2D dislocation field theory are given by

$$\ell_1^2 = \frac{c}{2\mu(1+\nu)}, \quad (27)$$

$$\ell_2^2 = \frac{c}{4} \left(\frac{1}{\mu} + \frac{1}{\gamma} \right) = \frac{c(\mu + \gamma)}{4\mu\gamma}. \quad (28)$$

They fulfill the relation

$$\ell_2^2 = \frac{(\mu + \gamma)(1 + \nu)}{2\gamma} \ell_1^2. \quad (29)$$

The inhomogeneous parts Φ^0 and Ψ^0 in Eqs. (25) and (26) are given by Eqs. (A.14) and (A.15).

The solutions of Eqs. (25) and (26) are (see also [11])

$$\Phi = -\frac{A}{2} \partial_y \left\{ r^2 \ln r + 4 \ell_1^2 \left[\ln r + K_0 \left(\frac{r}{\ell_1} \right) \right] \right\}, \quad (30)$$

$$\Psi = \frac{B}{2} \partial_x \left\{ r^2 \ln r + 4 \ell_2^2 \left[\ln r + K_0 \left(\frac{r}{\ell_2} \right) \right] \right\}. \quad (31)$$

where K_n denotes the modified Bessel function of the second kind and of order n and the pre-factors are given by

$$A = \frac{\mu(1+\nu)b}{2\pi}, \quad B = \frac{\mu\gamma b}{\pi(\mu + \gamma)}. \quad (32)$$

Substituting the stress functions (30) and (31) into the stress function ansatz (24),

the following components of the force stress tensor follow

$$\sigma_{xx} = -\frac{y}{r^4} \left\{ A \left[(y^2 + 3x^2) + \frac{4\ell_1^2}{r^2} (y^2 - 3x^2) - 2y^2 \frac{r}{\ell_1} K_1\left(\frac{r}{\ell_1}\right) - 2(y^2 - 3x^2) K_2\left(\frac{r}{\ell_1}\right) \right] \right. \\ \left. - B \left[(x^2 - y^2) - \frac{4\ell_2^2}{r^2} (3x^2 - y^2) + 2x^2 \frac{r}{\ell_2} K_1\left(\frac{r}{\ell_2}\right) - 2(y^2 - 3x^2) K_2\left(\frac{r}{\ell_2}\right) \right] \right\}, \quad (33)$$

$$\sigma_{yy} = -\frac{y}{r^4} \left\{ A \left[(y^2 - x^2) - \frac{4\ell_1^2}{r^2} (y^2 - 3x^2) - 2x^2 \frac{r}{\ell_1} K_1\left(\frac{r}{\ell_1}\right) + 2(y^2 - 3x^2) K_2\left(\frac{r}{\ell_1}\right) \right] \right. \\ \left. + B \left[(x^2 - y^2) - \frac{4\ell_2^2}{r^2} (3x^2 - y^2) + 2x^2 \frac{r}{\ell_2} K_1\left(\frac{r}{\ell_2}\right) + 2(3x^2 - y^2) K_2\left(\frac{r}{\ell_2}\right) \right] \right\}, \quad (34)$$

$$\sigma_{xy} = \frac{x}{r^4} \left\{ A \left[(x^2 - y^2) - \frac{4\ell_1^2}{r^2} (x^2 - 3y^2) - 2y^2 \frac{r}{\ell_1} K_1\left(\frac{r}{\ell_1}\right) + 2(x^2 - 3y^2) K_2\left(\frac{r}{\ell_1}\right) \right] \right. \\ \left. + B \left[(x^2 + 3y^2) + \frac{4\ell_2^2}{r^2} (x^2 - 3y^2) - 2x^2 \frac{r}{\ell_2} K_1\left(\frac{r}{\ell_2}\right) - 2(x^2 - 3y^2) K_2\left(\frac{r}{\ell_2}\right) \right] \right\}, \quad (35)$$

$$\sigma_{yx} = \frac{x}{r^4} \left\{ A \left[(x^2 - y^2) - \frac{4\ell_1^2}{r^2} (x^2 - 3y^2) - 2y^2 \frac{r}{\ell_1} K_1\left(\frac{r}{\ell_1}\right) + 2(x^2 - 3y^2) K_2\left(\frac{r}{\ell_1}\right) \right] \right. \\ \left. - B \left[(x^2 - y^2) - \frac{4\ell_2^2}{r^2} (x^2 - 3y^2) - 2y^2 \frac{r}{\ell_2} K_1\left(\frac{r}{\ell_2}\right) + 2(x^2 - 3y^2) K_2\left(\frac{r}{\ell_2}\right) \right] \right\}. \quad (36)$$

The trace of the stress tensor is

$$\sigma_{kk} = -2A \frac{y}{r^2} \left[1 - \frac{r}{\ell_1} K_1\left(\frac{r}{\ell_1}\right) \right] \quad (37)$$

and the skew-symmetric part of the force stress tensor reads

$$\sigma_{[xy]} = B \frac{x}{r^2} \left[1 - \frac{r}{\ell_2} K_1\left(\frac{r}{\ell_2}\right) \right]. \quad (38)$$

It is worth noting that all the components of the force stress tensor (33)–(38) are non-singular and finite everywhere and they agree with the force stresses of an edge dislocation calculated in the plane strain problem using the framework of three-dimensional dislocation gauge theory [11]. Only the pre-factor A and the pre-factor of the trace of the stress tensor are slightly different due to plane strain problem of an edge dislocation where $\sigma_{zz} \neq 0$ (see [11]).

Substituting Eqs. (33)–(38) into Eq. (18), the components of the elastic distortion

tensor are obtained

$$\begin{aligned} \beta_{xx} = & -\frac{y}{r^4} \left\{ \frac{A}{2\mu} \left[(y^2 + 3x^2) + \frac{4\ell_1^2}{r^2} (y^2 - 3x^2) - 2y^2 \frac{r}{\ell_1} K_1\left(\frac{r}{\ell_1}\right) - 2(y^2 - 3x^2) K_2\left(\frac{r}{\ell_1}\right) \right] \right. \\ & - \frac{B}{2\mu} \left[(x^2 - y^2) - \frac{4\ell_2^2}{r^2} (3x^2 - y^2) + 2x^2 \frac{r}{\ell_2} K_1\left(\frac{r}{\ell_2}\right) - 2(y^2 - 3x^2) K_2\left(\frac{r}{\ell_2}\right) \right] \\ & \left. - \frac{\nu b}{2\pi} r^2 \left[1 - \frac{r}{\ell_1} K_1\left(\frac{r}{\ell_1}\right) \right] \right\}, \end{aligned} \quad (39)$$

$$\begin{aligned} \beta_{yy} = & -\frac{y}{r^4} \left\{ \frac{A}{2\mu} \left[(y^2 - x^2) - \frac{4\ell_1^2}{r^2} (y^2 - 3x^2) - 2x^2 \frac{r}{\ell_1} K_1\left(\frac{r}{\ell_1}\right) + 2(y^2 - 3x^2) K_2\left(\frac{r}{\ell_1}\right) \right] \right. \\ & + \frac{B}{2\mu} \left[(x^2 - y^2) - \frac{4\ell_2^2}{r^2} (3x^2 - y^2) + 2x^2 \frac{r}{\ell_2} K_1\left(\frac{r}{\ell_2}\right) + 2(3x^2 - y^2) K_2\left(\frac{r}{\ell_2}\right) \right] \\ & \left. - \frac{\nu b}{2\pi} r^2 \left[1 - \frac{r}{\ell_1} K_1\left(\frac{r}{\ell_1}\right) \right] \right\}, \end{aligned} \quad (40)$$

$$\begin{aligned} \beta_{xy} = & \frac{x}{r^4} \left\{ \frac{A}{2\mu} \left[(x^2 - y^2) - \frac{4\ell_1^2}{r^2} (x^2 - 3y^2) - 2y^2 \frac{r}{\ell_1} K_1\left(\frac{r}{\ell_1}\right) + 2(x^2 - 3y^2) K_2\left(\frac{r}{\ell_1}\right) \right] \right. \\ & + \frac{B}{2\mu} \left[2y^2 + \frac{4\ell_2^2}{r^2} (x^2 - 3y^2) - (x^2 - y^2) \frac{r}{\ell_2} K_1\left(\frac{r}{\ell_2}\right) - 2(x^2 - 3y^2) K_2\left(\frac{r}{\ell_2}\right) \right] \\ & \left. + \frac{B}{2\gamma} r^2 \left[1 - \frac{r}{\ell_2} K_1\left(\frac{r}{\ell_2}\right) \right] \right\}, \end{aligned} \quad (41)$$

$$\begin{aligned} \beta_{yx} = & \frac{x}{r^4} \left\{ \frac{A}{2\mu} \left[(x^2 - y^2) - \frac{4\ell_1^2}{r^2} (x^2 - 3y^2) - 2y^2 \frac{r}{\ell_1} K_1\left(\frac{r}{\ell_1}\right) + 2(x^2 - 3y^2) K_2\left(\frac{r}{\ell_1}\right) \right] \right. \\ & + \frac{B}{2\mu} \left[2y^2 + \frac{4\ell_2^2}{r^2} (x^2 - 3y^2) - (x^2 - y^2) \frac{r}{\ell_2} K_1\left(\frac{r}{\ell_2}\right) - 2(x^2 - 3y^2) K_2\left(\frac{r}{\ell_2}\right) \right] \\ & \left. - \frac{B}{2\gamma} r^2 \left[1 - \frac{r}{\ell_2} K_1\left(\frac{r}{\ell_2}\right) \right] \right\}. \end{aligned} \quad (42)$$

The elastic dilatation reads

$$\beta_{kk} = -\frac{(1-\nu)b}{2\pi} \frac{y}{r^2} \left[1 - \frac{r}{\ell_1} K_1\left(\frac{r}{\ell_1}\right) \right]. \quad (43)$$

In addition the elastic rotation is

$$\beta_{[xy]} = \frac{\mu b}{2\pi(\mu + \gamma)} \frac{x}{r^2} \left[1 - \frac{r}{\ell_2} K_1\left(\frac{r}{\ell_2}\right) \right]. \quad (44)$$

In Eqs. (43) and (44) it can be seen that ℓ_1 and ℓ_2 are the characteristic lengths for the elastic dilatation and elastic rotation, respectively. The two characteristic lengths of our model should be estimated by using data from experiments: ℓ_1 from the profile of the elastic dilatation field and ℓ_2 from the profile of the elastic rotation field. The elastic dilatation field (43) and the elastic rotation field (44) are non-singular. Their extremum values are: $|\beta_{kk}(0, y)| \simeq 0.399(1-\nu)b/[2\pi\ell_1]$ at $|y| \simeq 1.114\ell_1$ and $|\beta_{[xy]}(x, 0)| \simeq 0.399\mu b/[2\pi(\mu + \gamma)\ell_2]$ at $|x| \simeq 1.114\ell_2$. In this way, the two material moduli γ and c may be determined. ℓ_2 can be determined from the position of the maximum of the

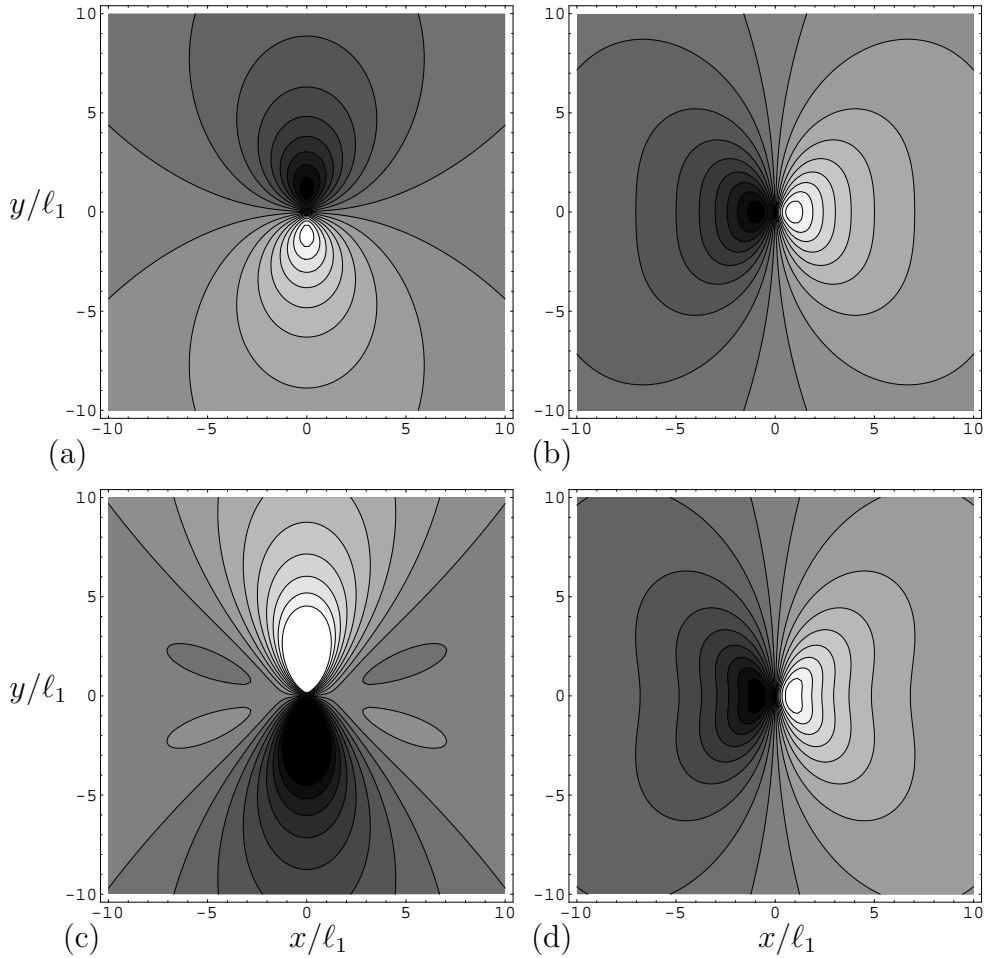


Figure 1: Elastic distortion contours of an edge dislocation near the dislocation point: (a) β_{xx} , (b) β_{xy} , (c) β_{yy} , (d) β_{yx} with the values: $\nu = 0.12$, $\mu = 9.95 \text{ eV/\AA}^2$ and $\gamma = 6\mu$.

elastic rotation, and γ from the maximum value of the elastic rotation. If l_2 and γ are determined, c can be computed from Eq. (28) and l_1 can be obtained from Eqs. (27) or (29). Using the elastic rotation $\beta_{[xy]}$, the new material parameters γ , c , l_1 , and l_2 may be determined. Thus, l_1 and l_2 may be used as fitting parameters in order to compare the experimental measurement with the presented theoretical model. In such a manner, the numerical values of the characteristic lengths may be determined from the experimental strain curves.

The elastic distortion fields (39)–(42) are plotted in Figs. 1 and 2. For the plots we used the relation (29) and the values: $\nu = 0.12$, $\mu = 9.95 \text{ eV/\AA}^2$ at 300 K [2] and $\gamma = 6\mu$. Fig. 1 shows the contours of the elastic distortion fields. The spatial distribution of the elastic distortion fields near the dislocation point is presented in Fig. 2. Fig. 2 demonstrates that the elastic distortion fields are non-singular. Thus, there is no singularity at the dislocation point. It can be seen in Fig. 1(a) that the elastic strain β_{xx} does not predict a 4-lobed strain field or strain field of butterfly shape as present in the classical isotropic elastic dislocation theory [18]. Moreover, it shows exactly the shape as measured recently in [1] (compare Fig. 1(a) in the present paper with Figs. S12(h) and S13 in the supplementary

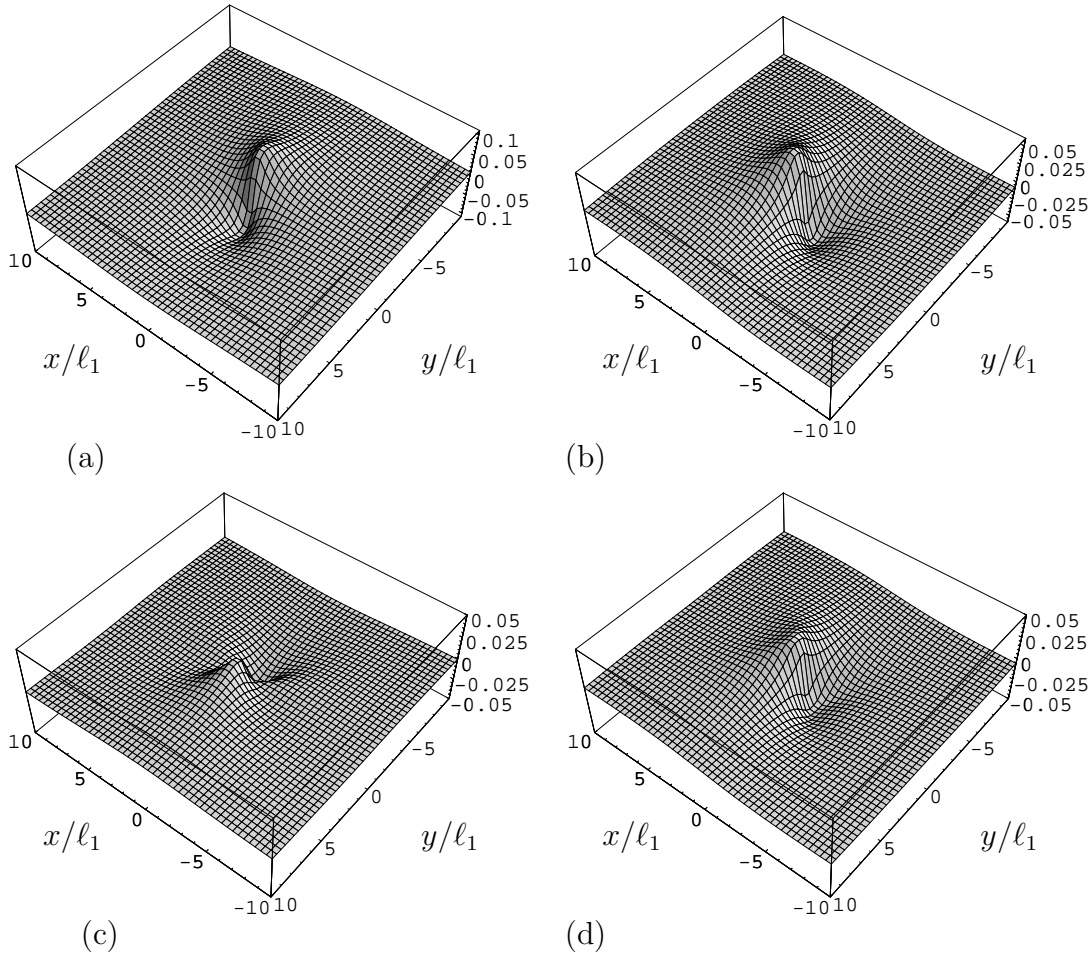


Figure 2: Elastic distortion of an edge dislocation in units of b : (a) β_{xx} , (b) β_{xy} , (c) β_{yy} , (d) β_{yx} with the values: $\nu = 0.12$, $\mu = 9.95 \text{ eV/\AA}^2$ and $\gamma = 6\mu$.

materials of [1]). In general, the elastic distortion fields have no artificial singularities in the core region and extremum values occur at a short distance away from the dislocation point (see Fig. 2).

Using the elastic distortion (39)–(42) in terms of the stress functions Φ and Ψ , we obtain for the dislocation density vector of an edge dislocation

$$\alpha_x = -\frac{1}{2\mu(1+\nu)} \partial_y \Delta \Phi + \frac{\mu + \gamma}{4\mu\gamma} \partial_x \Delta \Psi, \quad (45)$$

$$\alpha_y = \frac{1}{2\mu(1+\nu)} \partial_x \Delta \Phi + \frac{\mu + \gamma}{4\mu\gamma} \partial_y \Delta \Psi. \quad (46)$$

Differentiating and using the Eqs. (25) and (26), the non-vanishing expressions are obtained

$$\alpha_x = \frac{b}{4\pi} \left\{ \frac{1}{\ell_1^2} K_0\left(\frac{r}{\ell_1}\right) + \frac{1}{\ell_2^2} K_0\left(\frac{r}{\ell_2}\right) - \frac{x^2 - y^2}{r^2} \left[\frac{1}{\ell_1^2} K_2\left(\frac{r}{\ell_1}\right) - \frac{1}{\ell_2^2} K_2\left(\frac{r}{\ell_2}\right) \right] \right\}, \quad (47)$$

$$\alpha_y = -\frac{b}{2\pi} \frac{xy}{r^2} \left[\frac{1}{\ell_1^2} K_2\left(\frac{r}{\ell_1}\right) - \frac{1}{\ell_2^2} K_2\left(\frac{r}{\ell_2}\right) \right]. \quad (48)$$

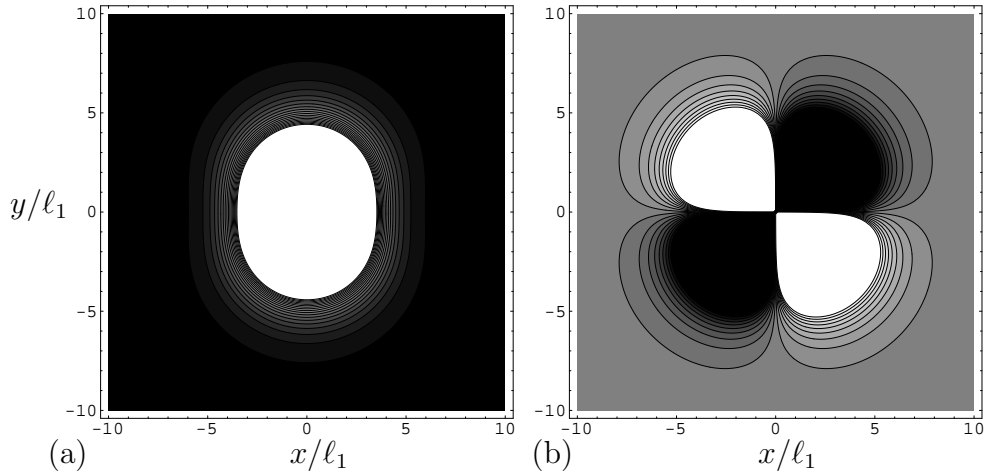


Figure 3: Contour plots of the dislocation density vector of an edge dislocation near the dislocation point: (a) α_x , (b) α_y with the values: $\nu = 0.12$, $\mu = 9.95 \text{ eV/\AA}^2$ and $\gamma = 6\mu$ (in units of $b/[4\pi]$).

It is worth noting that the component (48), which is usually the dislocation density of an edge dislocation with Burgers vector b_y , is non-zero. The components (47) and (48) are necessary to fulfill the dislocation equilibrium condition (15). It has been noted that these non-vanishing components of the dislocation density vector do not possess cylindrical symmetry due to the K_2 -terms (see Fig. 3). Since an edge dislocation is lacking cylindrical symmetry around the dislocation point two length scales, ℓ_1 and ℓ_2 , are needed for a proper modelling of the dislocation core of an edge dislocation.

Using the components (47) and (48) of the dislocation density vector, the Burgers vector is calculated as

$$\begin{aligned}
 b(r) &= \oint (\beta_{xx} dx + \beta_{xy} dy) = \int_0^{2\pi} \int_0^r \alpha_x(r', \phi') r' dr' d\phi' \\
 &= b \left\{ 1 - \frac{1}{2} \left[\frac{r}{\ell_1} K_1\left(\frac{r}{\ell_1}\right) + \frac{r}{\ell_2} K_1\left(\frac{r}{\ell_2}\right) \right] \right\}, \tag{49}
 \end{aligned}$$

$$0 = \oint (\beta_{yx} dx + \beta_{yy} dy) = \int_0^{2\pi} \int_0^r \alpha_y(r', \phi') r' dr' d\phi'. \tag{50}$$

Thus, it can be seen that the dislocation density (48) does not contribute to the Burgers vector. Only the K_0 -terms in (47) give a contribution to the Burgers vector (49). The effective Burgers vector (49) is plotted in Fig. 4. In Fig. 4, it can be seen that the effective Burgers vector $b(r)$ differs from the constant Burgers vector b in the region from $r = 0$ up to $r = 6\ell_1$.

Last but not least, we have to mention that all the expressions for the elastic distortion tensor, dislocation density vector, and the effective Burgers vector of an edge dislocation in graphene given in [19] are mistaken. The corresponding expressions calculated in this paper are the correct ones.

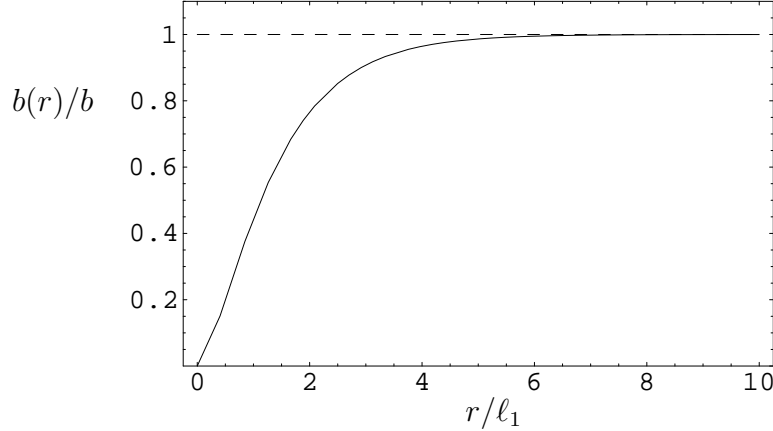


Figure 4: The modified Burgers vector of an edge dislocation $b(r)/b$ with the values: $\nu = 0.12$, $\mu = 9.95 \text{ eV}/\text{\AA}^2$ and $\gamma = 6\mu$ (solid).

4 Conclusions

In this paper we have developed a systematic dislocation continuum theory in 2D. We have used this theory for dislocations in graphene. We have calculated the stress and elastic distortion fields, which are non-singular due to a straightforward regularization. The calculated contour plots of the elastic distortion tensor agree well with experimental data [1]. The theory contains four material moduli and two characteristic length scales. The obtained results are useful for nano-mechanics of 2D materials (e.g., graphene). The results are especially important for the study of dislocations in monolayer graphene or other 2D materials.

Acknowledgement

The author gratefully acknowledges the grants from the Deutsche Forschungsgemeinschaft (Grant Nos. La1974/2-1, La1974/3-1).

A Appendix: Edge dislocation in 2D asymmetric elasticity

In the case of edge dislocations, the equations of incompatibility in 2D take the form

$$\alpha_x^0 = \beta_{xy,x}^0 - \beta_{xx,y}^0, \quad (\text{A.1})$$

$$\alpha_y^0 = \beta_{yy,x}^0 - \beta_{yx,y}^0. \quad (\text{A.2})$$

We use the following combinations [20]

$$A_1 := \alpha_{y,x}^0 - \alpha_{x,y}^0 = \beta_{yy,xx}^0 + \beta_{xx,yy}^0 - \beta_{xy,xy}^0 - \beta_{yx,xy}^0, \quad (\text{A.3})$$

$$A_2 := -\alpha_{x,x}^0 - \alpha_{y,y}^0 = \beta_{yx,yy}^0 - \beta_{xy,xx}^0 + \beta_{xx,xy}^0 - \beta_{yy,xy}^0. \quad (\text{A.4})$$

Expressing the elastic distortions in terms of force stresses, we obtain

$$A_1 = \frac{1}{2\mu} \left(\sigma_{yy,xx}^0 + \sigma_{xx,yy}^0 - (\sigma_{xy,xy}^0 + \sigma_{yx,xy}^0) - \frac{\nu}{1+\nu} \Delta(\sigma_{xx}^0 + \sigma_{yy}^0) \right), \quad (\text{A.5})$$

$$A_2 = \frac{1}{2\mu} (\sigma_{xx,xy}^0 - \sigma_{yy,xy}^0) + \frac{\gamma - \mu}{4\mu\gamma} (\sigma_{xy,yy}^0 - \sigma_{yx,xx}^0) + \frac{\gamma + \mu}{4\mu\gamma} (\sigma_{yx,yy}^0 - \sigma_{xy,xx}^0). \quad (\text{A.6})$$

Because we deal with asymmetric force stresses we use a 2D stress function ansatz given by Mindlin for couple-stress theory [17]

$$\sigma_{ij}^0 = \begin{pmatrix} \partial_{yy}^2 \Phi^0 - \partial_{xy}^2 \Psi^0 & -\partial_{xy}^2 f^0 + \partial_{xx}^2 \Psi^0 \\ -\partial_{xy}^2 \Phi^0 - \partial_{yy}^2 \Psi^0 & \partial_{xx}^2 f^0 + \partial_{xy}^2 \Psi^0 \end{pmatrix}, \quad (\text{A.7})$$

where Φ^0 and Ψ^0 are stress functions of second order. The stress function ansatz (A.7) is the generalization of the stress function ansatz with the Airy stress function Φ^0 for symmetric stresses. If Ψ^0 is zero, (A.7) reduces to the usual expression for the stresses in terms of the Airy stress function Φ^0 . Equations (A.5) and (A.6) are reduced to the following 2D inhomogeneous bi-harmonic equations

$$\Delta\Delta \Phi^0 = 2\mu(1+\nu)A_1, \quad (\text{A.8})$$

$$\Delta\Delta \Psi^0 = -\frac{4\mu\gamma}{\mu+\gamma}A_2. \quad (\text{A.9})$$

Because we consider an edge dislocation located at $(x, y) = (0, 0)$ and with the Burgers vector $b = b_x$, the dislocation density vector has the form

$$\alpha_y^0 = 0, \quad \alpha_x^0 = b \delta(x)\delta(y). \quad (\text{A.10})$$

In this manner, we obtain

$$\Delta\Delta \Phi^0 = -2\mu(1+\nu)b \partial_y[\delta(x)\delta(y)], \quad (\text{A.11})$$

$$\Delta\Delta \Psi^0 = \frac{4\mu\gamma b}{\mu+\gamma} \partial_x[\delta(x)\delta(y)]. \quad (\text{A.12})$$

Since the 2D Green function of the bi-harmonic equation is

$$\Delta\Delta G = \delta(x)\delta(y), \quad G = \frac{1}{8\pi} r^2 \ln r \quad (\text{A.13})$$

the solutions of (A.11) and (A.12) are the following Airy stress functions [21]

$$\Phi^0 = -\frac{\mu(1+\nu)b}{4\pi} \partial_y(r^2 \ln r) \quad (\text{A.14})$$

$$\Psi^0 = \frac{\mu\gamma b}{2\pi(\mu+\gamma)} \partial_x(r^2 \ln r). \quad (\text{A.15})$$

(A.14) is the well-known Airy stress function for an edge dislocation in 2D with Burgers vector b_x . (A.15) looks like an Airy stress function for an edge dislocation with Burgers vector b_y with a different pre-factor.

References

- [1] J.H. Warner, E.R. Margine, M. Mukai, A.W. Robertson, F. Giustino, and A.I. Kirkland, Dislocation-Driven Deformations in Graphene, *Science* **337** (2012) 209–212, [Supplementary Materials].
- [2] K.V. Zakharchenko, M.I. Katsnelson, and A. Fasolino, Finite Temperature Lattice Properties of Graphene beyond the Quasiharmonic Approximation, *Phys. Rev. Lett.* **102** (2009) 046808 [4 pages].
- [3] O.V. Yazyev and S.G. Louie, Topological defects in graphene: Dislocations and grain boundaries, *Phys. Rev. B* **81** (2010) 195420 [7 pages].
- [4] S. Chen and D.C. Chrzan, Continuum theory of dislocations and buckling in graphene, *Phys. Rev. B* **84** (2011) 214103 [5 pages].
- [5] M.A.H. Vozmediano, M.I. Katsnelson, and F. Guinea, Gauge fields in graphene, *Physics Reports* **496** (2010) 109–148.
- [6] F. de Juan, A. Cortijo, and M.A.H. Vozmediano, Dislocations and torsion in graphene and related systems, *Nuclear Physics B* **828** (2010) 625–637.
- [7] A. Kadić and D.G.B. Edelen, *A Gauge Theory of Dislocations and Disclinations*, Springer, Berlin (1983).
- [8] D.G.B. Edelen and D.C. Lagoudas, *Gauge Theory and Defects in Solids*, North-Holland, Amsterdam (1988).
- [9] M. Lazar, Dislocation theory as a 3-dimensional translation gauge theory, *Ann. Phys. (Leipzig)* **9** (2000) 461–473.
- [10] M. Lazar and C. Anastassiadis, The gauge theory of dislocations: conservation and balance laws, *Phil. Mag.* **88** (2008) 1673–1699.
- [11] M. Lazar and C. Anastassiadis, The gauge theory of dislocations: static solutions of screw and edge dislocations, *Phil. Mag.* **89** (2009) 199–231.
- [12] M. Lazar, On the Higgs mechanism and stress functions in the translational gauge theory of dislocations, *Physics Letters A* **373** (2009) 1578–1582.
- [13] M. Lazar and F.W. Hehl, Cartan’s spiral staircase in physics and, in particular, in the gauge theory of dislocations, *Foundations of Physics* **40** (2010) 1298–1325.
- [14] E. Agiasofitou and M. Lazar, On the nonlinear continuum theory of dislocations: a gauge field theoretical approach, *Journal of Elasticity* **99** (2010) 163–178.
- [15] E.W. Mielke, F. Gronwald, Y.N. Obukhov, T. Tresguerres, and F.W. Hehl, Towards complete integrability of two dimensional Poincaré gauge theory, *Phys. Rev. D* **48** (1993) 3648–3662.

- [16] F.W. Hehl, J.D. McCrea, E.W. Mielke, and Y. Ne'eman, Metric-affine gauge theory of gravity: Field equations, Noether identities, world spinors, and breaking of dilation invariance, *Phys. Rep.* **258** (1995) 1–171.
- [17] R.D. Mindlin, Influence of couple-stresses on stress concentrations, *Exper. Mech.* **3** (1963) 1–7.
- [18] J.P. Hirth and J. Lothe, *Theory of Dislocations*, 2nd edition, John Wiley, New York (1982).
- [19] L.L. Bonilla and A. Carpio, Strain and rotation fields of dislocations in graphene, (2012) [arXiv:1207.5675]
- [20] W. Nowacki, *Theory of Asymmetric Elasticity*, Pergamon Press, Oxford (1986).
- [21] E. Kröner, *Continuum Theory of Defects*, in: *Physics of Defects* (Les Houches, Session 35), R. Balian et al., eds., North-Holland, Amsterdam (1981) p. 215.